Egypt. J. Chem. **Vol. 65,** No. 10 pp. 647 - 655 (2022)

Egyptian Journal of Chemistry

http://ejchem.journals.ekb.eg/

Synthesis of cubic p-NiO/n-In_2O_3 heterostructure as efficient photocatalyst for degradation of apramycin: Optimization of operating conditions

Sara Karim Dizani[1], Leila Torkian[2], Zahra Khodadadi[3,*], Reza Fazaeli[4], Saeed Safa[5]

[1] *Department of applied chemistry, South Tehran Branch, Islamic Azad University, Tehran, Iran (Email: S.dizanii@gmail.com)*

[2]*Department of applied chemistry, South Tehran Branch, Islamic Azad University, Tehran, Iran, (Email: ltorkian@gmail.com)*

[3,*] *Corresponding author: Department of applied chemistry, South Tehran Branch, Islamic Azad University, Tehran, Iran (Email: za_khd@yahoo.com)*

[4] *Department of Chemical engineering, Faculty of engineering, South Tehran Branch, Islamic Azad University, Tehran, Iran (Email: r_fazaeli@azad.ac.ir)*

[5] *Department of applied chemistry, South Tehran Branch, Islamic Azad University, Tehran, Iran (Email:safa1493@gmail.com)*

Abstract

In this reasarch, Indium oxide (In_2O_3), nickel oxide (NiO) and NiO/In_2O_3 heterostructure were synthesized and characterized using X-ray diffraction (XRD), Fourier-transform infrared spectroscopy (FTIR), scanning electron microscope (SEM), energy dispersive X-ray spectrometry (EDS)/Map, Brunauer, Emmett, Teller (BET)/Barrett, Joyner, Halenda (BJH) and UV–vis diffuse reflectance spectroscopy (DRS) techniques. The photocatalytic degradation of Apramycin (APR) from aqueous solutions studied by photocatalysts synthesized. In order to investigate the effect of parameters in degradation of APR, were used from response surface methodology (RSM). The effect of NiO/In_2O_3 (0.5:1) catalyst mass (g), time (min) and pH on degradation of APR evaluated. Design expert software is the best point to achieve the maximum degradation efficiency of APR 99.99%, in optimum conditions at pH 5.01, time 27.54 (min), mass of catalyst 0.03 (g).

Keywords: NiO/In_2O_3; Photocatalyst; Antibiotic; Apramycin; Response surface methodology

Introduction

Water pollution in surface and groundwater sources can cause problems for human health. Pollution enters the environment mainly through human activities and production processes in factories. One of these pollutants is antibiotics, which have a special place in the treatment of humans and animals due to their high consumption [1]. Due to the lack of water and the occurrence of environmental problems caused by the discharge of sewage and effluents into the receiving water, wastewater treatment and the possibility of reusing it has been considered. This operation is performed using physical, chemical and biological processes and continues until the quality of the effluent reaches the level of existing standards [2]. Antibiotics are not fully metabolized in the body after use and remain active after excretion. Apramycin (APR) is an important class of non-degradable antibiotics used in humans and animals. APR contains a unique member of nebramycins. Used only for animals, which was reported in veterinary medicine in several countries in the early 1980s. Due to its broad-spectrum activity against gram-positive and gram-negative bacteria, APR can be widely used in animals as an intestinal disinfectant and as an antibacterial for systemic use. This antibiotic is prescribed for pigs, calves, rabbits and lambs to treat clibacillus, salmonellosis, bacterial enteritis and also to prevent Escherichia coli septicemia in poultry. In addition, unlike other aminoglycosides, it exhibits potent activity against a wide range of clinical pathogens. Thus, it is introduced as a candidate drug for the treatment of bacterial infectious diseases [4,5]. Methods used to removal APR and other antibiotics to date include separation membranes[5], ozonation [6], nanofiltration [7], advanced oxidation processes[8], photocatalytic [9-14], and adsorption [15]. One of these important methods is absorption. Evidence shows that removal by physical methods is not efficient enough to remove antibiotics, and chemical treatment leads to the

*Corresponding author e-mail: za_khd@yahoo.com

Receive Date: 11 December 2021, Revise Date: 15 January 2022, Accept Date: 21 February 2022

DOI: 10.21608/EJCHEM.2022.110726.5044

©2022 National Information and Documentation Center (NIDOC)

production of harmful by-products. Therefore, photocatalytic processes are a suitable tool for the analysis and elimination of drugs. In recent years, metal oxide nanostructures have received increasing attention in both the basic sciences and the applied sciences, and among them In_2O_3 is one of the semiconductor materials with many properties and applications [13,14]. In_2O_3 is a semiconductor n- type with band gap of about 3.75 eV. In_2O_3 has many applications in solar cell, chemical and biological sensors and as a photocatalyst [16]. NiO has also attracted much scientific research due to its magnetic and electronic properties. NiO semiconductor is a p-type which energy band gap has been experimentally obtained at 2.7-4 eV. NiO network defects play a key role in the amount of energy gap. Also, NiO is a promising material for applications in fuel cell, photocatalysts, electrochemical capacitors, etc. [17, 18]. The heterostructure design of p-NiO /n-In_2O_3 is interesting for studying their photocatalytic properties [19]. In recent years, the use of statistical methods to design experiments in various fields of science and engineering has been considered by researchers. Classical methods for achieving the optimal value in experiments have various disadvantages, the most important of which is the large number of experiments. Using a variety of test design methods such as Taguchi methods, RSM, etc. can eliminate these disadvantages. The application of these statistical methods has higher accuracy, less number of tests, less time and minimal cost of tests compared to conventional classical methods [20,23]. In this study, p-NiO/n-In_2O_3 heterostructure were synthesized. The degradation of APR was studied by photocatalysts. Then, we used BBD-based RSM to investigate the parameters affecting the photocatalytic degradation of APR and optimizing operating conditions. Also, 2, 3 and 4 parameter adsorption isotherms were studied.

Materials and Methods

Materials

Indium nitrate ($In(NO_3)_3{\cdot}4.5H_2O$, 99.5%), sucrose ($C_{12}H_{22}O_{11}$, 99.5%), urea (NH_2CONH_2, 99.9%), Nickel Chloride ($NiCl_2$), Sodium oxalate ($Na_2C_2O_4$), Ethylene Glycol was prepared by Sigma-Aldrich Company. Apramycin ($C_{21}H_{41}N_5O_{11}$ 20%) was prepared by Daru Life Co (Figure 1).

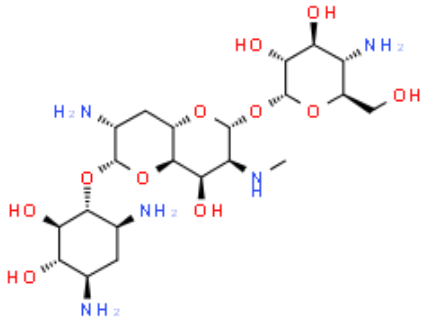

Fig. 1. End configuration of apramycin molecule.

Synthesis of In_2O_3

0.19 g of $In(NO)_3{\cdot}4.5H_2O$, 0.68 g of $C_{12}H_{22}O_{11}$ and 0.75 g of NH_2CONH_2 was poured into 15 mL of distilled water and placed on the stirrer for 1 h. The prepared solution was poured into a hydrothermal autoclave and placed at 180 ° C for 10 h. Then, the precipitate was washed with distilled water and then placed in the oven at 80 ° C for 30 min and in furnace at 600 ° C for 120 min [16].

Synthesis of NiO

0.15 g of $NiCl_2$, 0.03 g of $Na_2C_2O_4$ was poured into 40 mL of EG and placed on a stirrer for 2 h. The prepared solution was poured into a hydrothermal autoclave and placed at 160 °C for 18 h. The precipitate was washed with distilled water and then placed in an oven at 100 ° C for 30 min and in furnace at 500 ° C for 60 min.

Synthesis of p-NiO/n-In_2O_3 heterostructure

1 g of In_2O_3 with different amounts of NiO 0.3, 0.5, 0.7 g was poured into 50 mL of distilled water and after 24 h was placed in an oven at 100 ° C for 120 min.

Degradation of APR

Degradation of APR were performed in photoreactor under UV-C 64W (254 nm) irradiated for 2 h. 50 mL of APR with concentration of 25 mg/L at pH = 7 with 0.1 g of NiO/In_2O_3 catalysts with weight percentages of 0.3: 1, 0.5: 1 and 0.7: 1 was poured into beaker and placed in a photoreactor. The samples were centrifuged at 70,000 rpm. At that time, its absorption was measured by UV-visible spectroscopy at 310 nm.

Efficiency = $\frac{(A_0 - A_t)}{A_0} * 100$ (1)

Here, A_0 is the initial absorption of APR and A_t is its final absorption after reaction.

Design of experiments

In this research, RSM was used to model the degradation process. RSM is a powerful tool for

statistical modeling that performs the least number of experimental experiments according to the experimental design. RSM itself has different types and this statistical method can be used in different ways. One of its types is the BBD method, which is a quadratic design based on incomplete three-level factorial designs. This method can estimate the value of the parameters in a quadratic model, make the required designs, and calculate the amount of the non-conformance parameter.

This scheme allows the answers to be modeled by fitting a second-order polynomial, which can be expressed as the following equation:

$$Y = \beta_0 + \sum_{j=1}^{k} \beta_j X_j + \sum_{j=1}^{k} \beta_{jj} X_j^2 + \sum_{i} \sum_{<j=2}^{k} \beta_{ij} X_i X_j + e_i \quad (2)$$

First, 50 mL of APR solution with concentration of 25 (mg/L) was prepared at pH 5, 7 and 9. Then 0.01, 0.03 and 0.05 (g) p-NiO/n-In_2O_3 (0.5:1) was poured into APR solution and exposed to UV-C light for 5, 17.5 and 30 (min) Table 1.

Isotherm studies

50 mL of APR solution with different concentrations of 20-120 (mg/L) at pH=5 was prepared. Then, 0.03 (g) p-NiO/n-In_2O_3 (0.5:1) was poured into it and exposed to UV-C light for 30 min.

The photocatalytic degradation of APR by p-NiO/n-In_2O_3 (0.5:1) photocatalyst was investigated under UV-C irradiation with isothermal equations of 2, 3 and 4 parameters and was minimized by 3 types of errors. The calculated isotherms and errors are shown in Tables 2 and 3, respectively [24].

Using Equation (3), were calculated the values of q_e and C_e.

$$q_e = \frac{(C_0 - C_e)V}{W} \quad (3)$$

Here, q_e is the mass of pollutant adsorbed per unit mass of catalyst, C_0 and C_e are the initial and final concentrations of APR, respectively. V is the volume of APR solution (L) and W is the mass of the catalyst (g).

Table 1. Independent variables and their levels in the experimental.

Independent variables	Coded symbols	Levels
Mass of catalyst (g)	X_1	0.01, 0.03, 0.05
Time (min)	X_2	5 17.5 30
pH	X_3	5 7 9

Table 2. Lists of adsorption isotherms models.

Isotherm	Nonlinear form	Isotherm	Nonlinear form	Isotherm	Nonlinear form
2 Parameters Langmuir	$q_e = \frac{q_m b_L C_e}{1 + b_L C_e}$	3 Parameters Redlich-Peterson	$q_e = \frac{K_R C_e}{1 + a_R C_e^g}$	4 Parameters Fritz-Schlunder	$q_e = \frac{C C_e^{\alpha_{FS}}}{1 + D C_e^{\beta_{FS}}}$
Freundlich	$q_e = K_f C_e^{1/n}$	Khan	$q_e = \frac{q_S b_{KH} C_e}{(1 + b_{KH} C_e)^{a_{KH}}}$		
Tempkin	$q_e = B_T \ln A_T C_e$	Radke-Prausnitz	$q_e = \frac{a_{RP} r_{RP} C_e}{1 + r_R C_e^{B_{RP}}}$		

Table 3. Explanation of different error functions.

Error function	Abbreviation	Definition/expression
Hybrid fractional error function	HYBRID	$\frac{1}{n}\sum_{i=1}^{n}\left[\frac{(q_{\exp} - q_{cal})^2}{q_{\exp}}\right]_i$
Marquardt's percent standard deviation	MPSD	$\frac{1}{n}\sum_{i=1}^{n}\left(\frac{q_{e,\exp} - q_{e,cal}}{q_{e,\exp}}\right)_i^2$
Average relative error	ARE	$\frac{1}{n}\sum_{i=1}^{n}\left\lvert\frac{q_{\exp} - q_{cal}}{q_{\exp}}\right\rvert_i$

. Results and Discussion

In_2O_3, NiO and p-NiO/n-In_2O_3 catalyst was synthesized and analyzed by XRD technique (Fig. 2). The XRD pattern of In_2O_3 and NiO catalyst have a cubic phase [16, 17]. In p-NiO/n-In_2O_3 catalyst the XRD peak at 2θ of 30.58, 35.46, 51.02, and 60.66° and 37.25, 43.29, and 62.84° are related to In_2O_3 and NiO, respectively (Fig. 2).

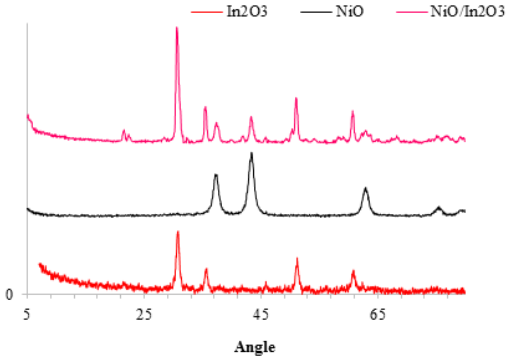

Fig 2. XRD pattern of In_2O_3, NiO and NiO/In_2O_3.

The vibrations of In_2O_3, NiO and p-NiO/n-In_2O_3 catalysts were investigated by FTIR spectroscopy. In the FTIR In_2O_3 peak, the absorption bands in the range of 600-800 cm^{-1} are assigned to the In-O bond. The peak at 2329.98 cm^{-1} is related to CO_2 uptake and the adsorption band at about 3435.62 cm^{-1} is corresponding to O-H traction. At the FTIR NiO, peaks at 432.37 and 471.03 cm^{-1} are assigned to the Ni-O bond. The bonds are 1639.94 and 3448.51 cm^{-1}, which are characteristic to O-H-O and O-H, respectively. In FTIR spectrum, p-NiO/n-In_2O_3 catalysts are in the range of 432.37 cm^{-1} for Ni-O, in the range of 600-800 cm^{-1} for the In-O bond, in the range of 2329.98 and 432.37 cm^{-1}, related to CO_2 and OH, respectively (Figure 3).

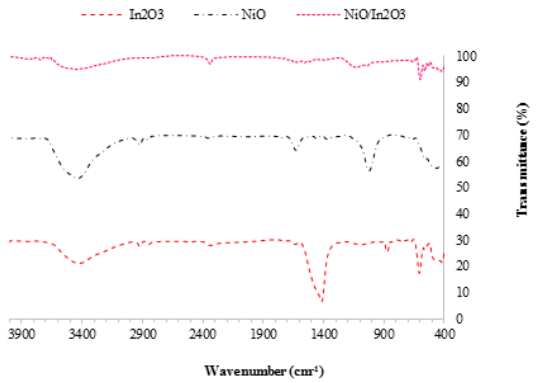

Fig. 3. FTIR spectrum of In_2O_3, NiO and NiO/In_2O_3 .

In_2O_3, NiO, and p-NiO/n-In_2O_3 were investigated by SEM, (Fig. 4). SEM results demonstrate that In_2O_3 and NiO particles have cubic and spherical morphology, respectively and are in nanoscale. Moreover, based on the results, NiO particles on the In_2O_3 cube are well loaded.

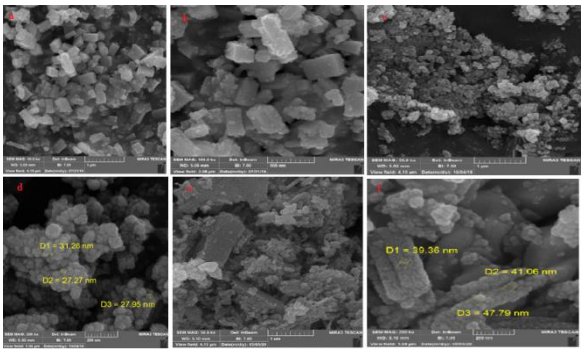

Fig. 4. SEM images of a) and b) In_2O_3, c) and d) NiO, e) and f) NiO/In_2O_3

The Xmap technique examines point-by-point a specific area of the sample. In this technique, EDS analysis is performed from a large number of points in a specified area and the results of this analysis are displayed as a series of colored dots. Each color represents an element. Where the amount of this element is greater, the number of dots with that particular color is greater. In p-NiO/n-In_2O_3 map images, the blue, red, and green dots indicate the presence of In, Ni, and O, respectively (Figure 5).
Based on the EDS results, the presence of O (28.02%), In(62.65%), and Ni (9.33%) elements in p-NiO/n-In_2O_3 (Fig 5. e).

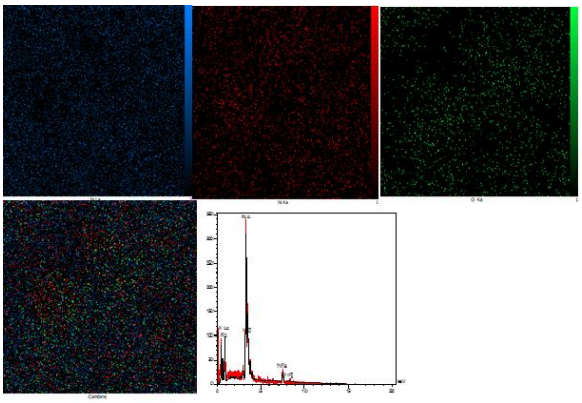

Fig .5. Map images of a) In, b) Ni, c) O, d) combine and e)EDS pattern of NiO/In$_2$O$_3$

BET specific surface measurement analysis is a physical analysis method for examining specific surface area and material porosity. This method, which is based on calculating the absorption and excretion of gases such as nitrogen, is a simple and inexpensive method that can be analyzed by estimating the surface area of the obtained materials. The results of BET/BJH for catalysts are demonstrate in Fig. 6 and Table 4. According the results, synthetic catalysts are of isotherm type IV. By loading NiO on In$_2$O$_3$, the surface area, pore volume and mean pore increased.

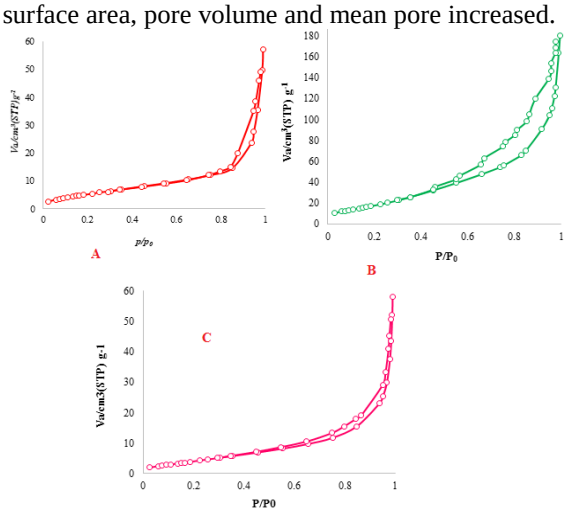

Fig. 6. N$_2$ adsorption-desorption isotherms of the a) In$_2$O$_3$, b) NiO and c) NiO/In$_2$O$_3$

Table 4. Results of BET/BJH analysis for various catalysts.

Catalyst	a_S, BET (m^2 g^{-1})	Total pore volume (cm^3 g^{-1})	Mean pore diameter (nm)
In_2O_3	20.37	0.087	17.18
NiO	64.88	0.25	15.83
NiO/In_2O_3	24.50	0.13	20.42

Whenever light with energy hν lands on a substance, it can pass through the layer, be reflected or absorbed, depending on the magnitude of its energy. If the energy of the landing photons is less than the band gap, it passes through and if it is higher, it is absorbed.

Using the absorption coefficient (α), the band gap of thin layers can be studied with the help of Tauc equation.

$(\alpha h\nu)^{1/n} = A\ (h\nu - E_g)$ (4)

The band gaps of In_2O_3, NiO and p-NiO/n-In_2O_3 were obtained as eV 3.6, 2.7, and 3.1 with Tauc equation, respectively (Fig. 7).

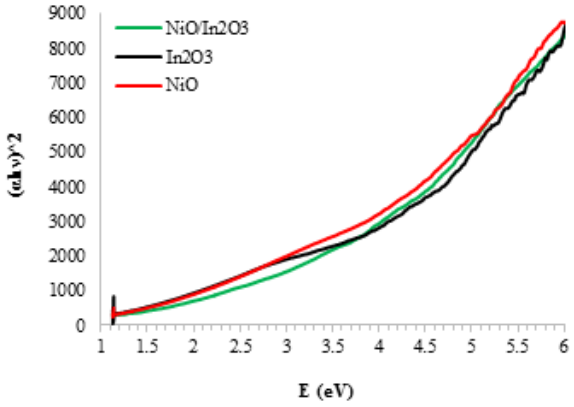

Fig 7. Band gap energies of In$_2$O$_3$, NiO and NiO/In$_2$O$_3$

Effect of NiO to In$_2$O$_3$ weight ratios on photocatalytic degradation

Based on the results, it can be seen that by increasing the amount of NiO photocatalyst from 0.3 to 0.5 g, the degradation efficiency increased from 80.45 to 98.16, but at values higher than 0.7 g, a decrease in efficiency is evident because with increasing the amount of electron photocatalyst the more cavities produced as a result of the more degradation process. This increase can occur through various mechanisms. The addition of NiO can increase the degradation activity through the load transfer mechanism between the conductor strips of the two semiconductors. On the other hand, adding 0.5 g of NiO to In$_2$O$_3$ increases the NiO diffusion and thus increases the active surface of the In$_2$O$_3$ substrate and increases the photocatalytic activity. However, in amounts greater than 0.5 g, as the particles agglomerate, the surface area decreases and as a result, the amount of degradation decreases. The reason for agglomeration of particles can be stated in their nano-dimensions because at the nanoscale, the surface energy increases and if in a solution with a certain amount, the number of nanoparticles increases from an optimal value, the surface energy instead of being spent on the pathway to increase photocatalytic activity is to agglomerate (Fig. 8).

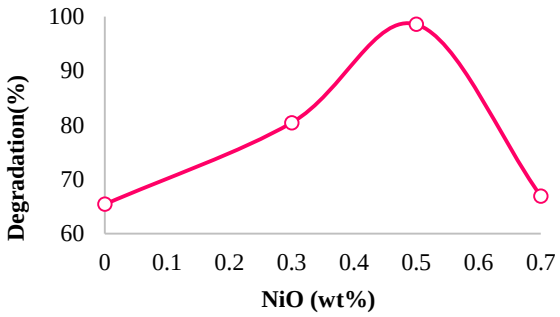

Fig 8. Effect of weight percentage of loaded NiO.

Statistical analysis

Statistical evaluation was performed by performing F-test and ANOVA analysis of variance of the quadratic model of RSM and the result is given in Table 5. ANOVA data confirm the accuracy of this quadratic model. Parameter F is a measure of the deviation of the data from the mean value. F-value for this model is 138.22, which indicates that the model is completely significant. On the other hand, the value of parameter R-Squared is 0.985 in accordance with Adj R-Squared 0.972 values, which indicates the accuracy of the model. Fig. 9 shows the disturbance diagram for photocatalytic degradation of APR. Based on the obtained results, it can be concluded that the pH parameter (parameter A) has the greatest effect on the photocatalytic degradation of APR.

Experimental data were studied with 2, 3 and 4 parametric isotherms and finally minimized by 3 error models (HYBRID, MPSD and ARE) (Table 6). The results of isothermal studies demonstrate that the Fritz-Schlunder isotherm with the least error with the experimental data of p-NiO/n-In_2O_3 photocatalytic degradation have the best fit (Table 7).

Table 5. The BBD for the 4 independent variables.

STD	Run	Mass of catalyst (g)	Time (min)	pH	Removal (%)
11	1	0.03	5.00	9.00	58.23
12	2	0.03	30.00	9.00	68.09
4	3	0.05	30.00	7.00	84.52
6	4	0.05	17.50	5.00	98.99
10	5	0.03	30.00	5.00	99.99
13	6	0.03	17.50	7.00	81.33
7	7	0.01	17.50	9.00	53.04
9	8	0.03	5.00	5.00	95.99
14	9	0.03	17.50	7.00	82.12
8	10	0.05	17.50	9.00	61.35
15	11	0.03	17.50	7.00	80.32
1	12	0.01	5.00	7.00	70.92
3	13	0.01	30.00	7.00	83.43
5	14	0.01	17.50	5.00	94.11
2	15	0.05	5.00	7.00	84.22

Effect of mass of catalyst and time

Two parameters of mass of catalyst and time on the degradation efficiency of APR was investigated by taking into the concentration of APR at 10 mg/L. Fig. 10 shows the effect of catalyst mass and time on degradation of APR as 2D and 3D. Based on the results, the degradation efficiency increases with the increase of catalyst mass and time. The p-NiO/n-In_2O_3 (0.5:1) photocatalyst is able to removal drugs from the water in a shorter period of time than other photocatalysts. This amount of adsorbent can be removed above 90% at concentrations of 100 mg/L (Fig. 10).

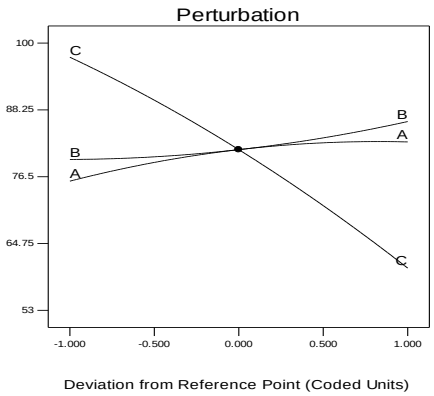

Fig 9. Perturbation plot for degradation of apramycin.

Effect mass of catalyst and pH

Two parameters of mass of catalyst and pH on degradation efficiency of APR was investigated by taking into the concentration of APR at 10 mg/L. The pH value plays an important role in the adsorption of particle ions by the NiO/In_2O_3 (0.5:1) catalyst. The pH affects the reaction between the catalyst and the adsorbent by changing the ionic state, and charging the catalyst surface. Fig. 11 illustrations the effect of catalyst mass and pH on degradation of APR as 2D and 3D. Based on the results, with increasing catalyst mass and decreasing pH, degradation efficiency of APR increases. Results showed that NiO/In_2O_3 (0.5:1) catalysts have a higher ability to degradation APR in the acidic pH. The surface charge of the NiO/In_2O_3 (0.5:1) catalyst becomes more negative with increasing pH, which in turn causes electrostatic reactions and as a result negatively charged APR will be less adsorbed when the pH of the solution is higher than the pH_{PZC} (pH = 8.5). Wet pH_{PZC} occurs under acidic conditions at the surface of the positive charge adsorbent, which is effective in the adsorption and degradation of drugs (Fig.11).

Effect of time and pH

Fig. 12 demonstrates the effect of time and pH on degradation of APR as 2D and 3D. Based on the results, the removal efficiency of the drug increases with increasing time and decreasing pH, as shown in Fig. 12. It is possible that in the early stages, the rate of degradation was so high that more than 90% of the drug was removed from the solution within 5 min. The experiments lasted up to 30 min and the results showed that the removal did not increase over time.

Table 6. ANOVA for analysis of variance and adequacy of the quadratic model.

Source	Sum of squares	Degree of freedom	Mean square	F-value	P-value Prob >F
Model	3031.32	9	336.81	138.22	< 0.0001 significant
A-Mass of catalyst	95.08	1	95.08	39.02	0.0015
B-Time	88.91	1	88.91	36.49	0.0018
C-pH	2751.71	1	2751.71	1129.26	< 0.0001
AB	37.27	1	37.27	15.30	0.0113
AC	2.94	1	2.94	1.21	0.3220
BC	8.58	1	8.58	3.52	0.1193
A^2	16.18	1	16.18	6.64	0.0496
B^2	9.56	1	9.56	3.92	0.1045
C^2	19.38	1	19.38	7.95	0.0371
Residual	12.18	5	2.44		
Lack of Fit	10.56	3	3.52	4.32	0.1936 not significant
Pure Error	1.63	2	0.81		
Cor Total	3043.51	14			

Table 7. Isotherms and error functions for NiO/In_2O_3.

Isotherm	isotherm parameter	Error & R^2	Error Value & R^2
Langmuir		HYBRID	77.189
q_m	123.21	MPSD	2.025
b_L	0.13	ARE	0.8853
		R^2	0.6542
Freundlich		HYBRID	3.218
K_f	2.7074E-08	MPSD	0.1357
N	0.3196	ARE	0.1696
		R^2	0.9740
Tempkin		HYBRID	11.773
B_T	0.0015	MPSD	0.1525
A_T	230.12	ARE	0.3328
		R^2	0.8872
Redlich-Peterson		HYBRID	27.0418
K_R	0.1995	MPSD	0.6173
a_R	3.6869	ARE	0.5856
G	0.2312	R^2	0.8086
Khan			
q_s	0.00005	HYBRID	4.1436
b_{KH}	0.530	MPSD	0.0862
a_{KH}	2.4958	ARE	0.2251
		R^2	0.9766
Radke-Prausnitz		HYBRID	4.1806
a_{RP}	6.098	MPSD	0.0485
r_{RP}	2740	ARE	0.1478
B_{RP}	1.710	R^2	0.9622
Fritz-Schlunder (IV)		HYBRID	1.4687
C	5.3194	MPSD	0.0017
D	3.4203	ARE	0.0045
α_{FS}	0.0001	R^2	0.9963
β_{FS}	0.097		

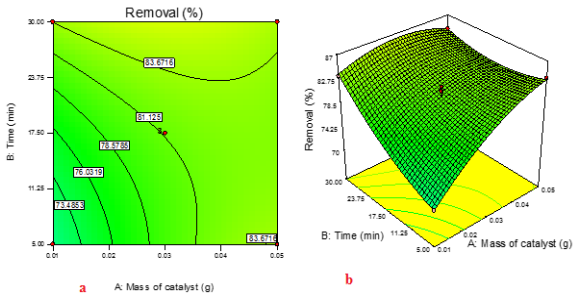

Fig 10. The effect of mass of catalyst and time for degradation apramycin a) Contour and b) 3D plot.

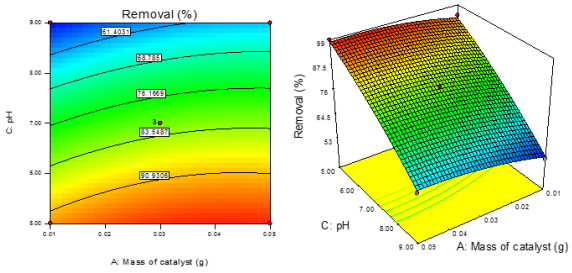

Fig 11. The effect of pH and mass of catalyst for degradation of apramycin a) Contour and b) 3D plot.

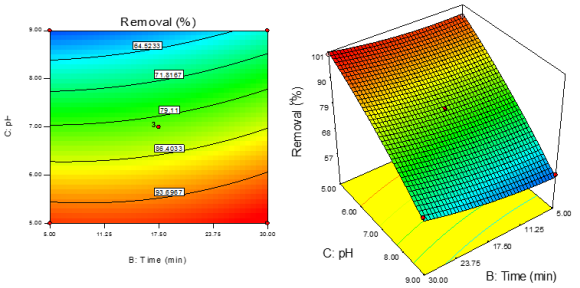

Fig 12. The effect of pH and time of apramycin for degradation of apramycin a) Contour and b) 3D plot.

Determining the optimal conditions

Finally, the software determined the best point to achieve the highest removal efficiency of APR, in optimal conditions with mass of catalyst 0.03 (g), time of 27.54 (min) and pH of 5.01, 99.99%.

Stability of p-NiO/n-In_2O_3 (0.5:1) heterostructure

One of the important factors in a catalyst's performance is the number of cycles of using that. For this purpose, after the degradation APR, p-NiO/n-In_2O_3 (0.5:1) heterostructure was separated, washed, and used for the same reaction. The results indicated that after 5 times of using the catalyst, the reaction oxidation decreased by about 8%.

Photodegradation process and mechanism of p-NiO/n-In_2O_3 (0.5:1) heterostructure

p-NiO/n-In_2O_3 (0.5:1) heterostructure photocatalysis were found to show high activity in organic compound degradation under UV-C light. Some factors involved in the p-NiO/n-In_2O_3 (0.5:1) heterostructure process, including surface area, crystallization, hierarchical architecture. APR degradation over the irradiated p-NiO/n-In_2O_3 (0.5:1) heterostructure in aqueous solution to the production of ·OH and H_2O. The valence band hole of p-NiO/n-In_2O_3 (0.5:1) heterostructure could oxidize water to produce ·OH and its conduction band electron could reduce O_2 to produce H_2O in the photocatalytic reaction.

Conclusion

Degradation of APR antibiotic by p-NiO/n-In_2O_3 (0.5:1) heterostructure in aqueous solutions were studied. Photocatalytic degradation of APR studied by catalysts prepared under UV-C light. Based on the results, the p-NiO/n-In_2O_3 (0.5:1) photocatalyst had the maximum degradation efficiency among the NiO, In_2O_3, p-NiO/n-In_2O_3 (0.5:1) photocatalysts. APR degradation by p-NiO/n-In_2O_3 (0.5:1) was investigated using RSM. The results showed that the statistical analysis of the software was highly accurate and also the effect of various parameters was well analyzed. Optimal conditions of photocatalytic degradation of APR at pH 5.0, time 27.54 (min), photocatalytic mass 0.03 (g) were obtained 99.99%. Isothermal studies shown that the Fritz-Schlander isotherm with the experimental data of p-NiO/n-In_2O_3 (0.5:1) photocatalytic degradation were the best fit.

REFERENCES

[1]. Donkadokula, N. Y., Kola, A. K., Naz, I., & Saroj, D. A review on advanced physico-chemical and biological textile dye wastewater treatment techniques. *Rev. Environ. Sci. Biotechnol*, 2020, vol. 19, pp. 543–560.

[2]. Khan, A. H., Khan, N. A., Ahmed, S., Dhingra, A., Singh, C. P., Khan, S. U., ... & Ali, I. Application of advanced oxidation processes followed by different treatment technologies for hospital wastewater treatment. . *J. Clean. Product*, 2020, vol. 269, pp. 12241.

[3]. Saadi, Z., Fazaeli, R., Vafajoo, L., & Naser, I. Adsorptive removal of apramycin antibiotic from aqueous solutions using Tween 80-and Triton X-100 modified clinoptilolite: experimental and fixed-bed modeling investigations. *Int. J. Environ. Health Res*, 2020, vol. 30, no. 5, pp. 558-583.

[4]. Quirke, J. C., Rajasekaran, P., Sarpe, V. A., Sonousi, A., Osinnii, I., Gysin, M., ... & Crich, D. Apralogs: Apramycin 5-O-Glycosides and Ethers with Improved Antibacterial Activity and Ribosomal Selectivity and Reduced Susceptibility to the Aminoacyltransferase (3)-IV Resistance Determinant. *J. Am. Chem. Soc*. 2020, vol. 142, no. 1, pp. 530-544.

[5]. Bojaran, M., Akbari, A., & Yunessnia lehi, A. Novel ultrafiltration membranes with the least fouling properties for the treatment of veterinary antibiotics in the pharmaceutical wastewater. *Polymer. Adv. Technol*. 2019, vol. 30, no. 7, pp. 1716-1723.

[6]. Iakovides, I. C., Michael-Kordatou, I., Moreira, N. F., Ribeiro, A. R., Fernandes, T., Pereira, M. F. R., ... & Fatta-Kassinos, D. Continuous ozonation of urban wastewater: Removal of antibiotics, antibiotic-resistant Escherichia coli and antibiotic resistance genes and phytotoxicity. *Water. Res*, 2019, vol. 159, pp. 333-347.

[7]. Lan, L., Kong, X., Sun, H., Li, C., & Liu, D. High removal efficiency of antibiotic resistance genes in swine wastewater via nanofiltration and reverse osmosis processes. *J. Environ. Manage*, 2019, vol. 231, pp. 439-445.

[8]. Anjali, R., & Shanthakumar, S. Insights on the current status of occurrence and removal of antibiotics in wastewater by advanced oxidation processes. *J. Environ. Manage*, 2019, vol. 246, pp. 51-62.

[9]. Fard, N. E., & Fazaeli, R. A novel kinetic approach for photocatalytic degradation of azo

dye with CdS and Ag/CdS nanoparticles fixed on a cement bed in a continuous- flow photoreactor. *International J. Chem. Kin*, 2016, vol. 48, no. 11, pp. 691-701.

[10]. Fard, N. E., Fazaeli, R., & Ghiasi, R. Band gap energies and photocatalytic properties of CdS and Ag/CdS nanoparticles for Azo dye degradation. *Chem. Eng. Technol*, 2016, vol. 39, no. 1, pp. 149-157.

[11]. Elmi Fard, N., & Fazaeli, R. Experimental design study of RB 255 photocatalytic degradation under visible light using synthetic Ag/TiO_2 nanoparticles: Optimization of experimental conditions. *Iran. J. Catal*, vol. 8, no. 2, pp. 133-141.

[12]. Fard, N. E., & Fazaeli, R. Optimization of Operating Parameters in Photocatalytic Activity of Visible Light Active Ag/TiO_2 Nanoparticles. *Russ. J. Physic. Chemistry A*, 2018, vol. 92, no. 13, pp. 2835-2846.

[13]. Fard, N. E., Fazaeli, R., Yousefi, M., & Abdolmohammadi, S. Oxidation of carbazole by shape-controllable Cu_2O on MWW catalysis. *Appl. Physic. A*, 2019, vol. 125, no. 9, pp. 632.

[14]. Fard, N. E., Fazaeli, R., Yousefi, M., & Abdolmohammadi, S. Morphology- Controlled Synthesis of CuO, CuO Rod/MWW Composite for Advanced Oxidation of Indole and Benzothiophene. *Chem. Select*, 2019, vol. 4, no. 33, pp. 9529-9539.

[15]. Ahangaran, E., Aghaie, H., & Fazaeli, R. Study of Amoxicillin Adsorption on the Silanized Multiwalled Carbon Nanotubes: Isotherms, Kinetics, and Thermodynamics Study. *Russ. J. Physic. Chem. A*, 2020, vol. 94, no. 13, pp. 2818-2828.

[16]. Karim Dizani, S., Torkian, L., Khodadadi, Z., Fazaeli, R., & Safa, S. Fabrication of cubic In_2O_3/Bi_2WO_6 and study of its photocatalytic performance in removal of florfenicol antibiotic from aqueous media: Experimental and molecular dynamic simulation. *J. Chin. Chem. Soc*. 2020, vol. 68, no. 2, pp. 263-273.

[17]. Goel, R., Jha, R., & Ravikant, C. Investigating the structural, electrochemical, and optical properties of p-type spherical nickel oxide (NiO) nanoparticles. *J. Physic. Chem. Solid*, 2020, vol. 144, pp. 109488.

[18]. Etefa, H. F., Imae, T., & Yanagida, M. Enhanced Photosensitization by Carbon Dots Co-adsorbing with Dye on p-Type Semiconductor (Nickel Oxide) Solar Cells. *Appl. Mater. Interfaces*.2020, vol. 12, no. 16, pp. 18596–18608.

[19]. Xuemei, H., Yukun, S., & Bo, B. Fabrication of cubic p-n heterojunction-like NiO/In_2O_3 composite microparticles and their enhanced gas sensing characteristics. J. Nanomater. 2016.

[20]. Kashi, N., Fard, N. E., & Fazaeli, R. Empirical modeling and CCD-based RSM optimization of Cd (II) adsorption from aqueous solution on clinoptilolite and bentonite. *Russ. J. Appl. Chem*, 2017, vol. 90(6), pp. 977-992.

[21]. Fazaeli, R., & Fard, N. E. Desulfurization of Gasoline Fuel via Photocatalytic Oxidation/Adsorption Using NaX Zeolite-Based under Mild Conditions: Process Optimization by Central Composite Design. *Russ. J. Appl. Chem*, 2020, vol. 93(7), pp. 973-982.

[22]. Fard, N. E., Fazaeli, R., Yousefi, M., & Abdolmohammadi, S. Oxidative Desulfurization of Dibenzothiophene Using M/TiO_2/MWW (M= Cu, Ag, and Au) Composite. *Russ. J. Physic. Chem*. A, 2021, vol. 95(1), pp. S23-S32

[23]. Fekra, S. S., Fard, N. E., & Fazaeli, R. Photocatalytic Degradation of Antibiotic Norfloxacin Aqueous Solution by Ce/Bi_2WO_6: Optimization and Simulation of Process by RSM. *Russ. J. Appl. Chem*, 2021, vol. 94(6), pp. 824-834.

[24]. Saadi, R., Saadi, Z., Fazaeli, R., & Fard, N. E. Monolayer and multilayer adsorption isotherm models for sorption from aqueous media. *Korea. J. Chem. Eng*, 2015, vol. 32(5), pp. 787-799.